Dynamic Taguchi Methods and Parameter Design as Applied in Barcode Scanning and Scanners

Nicholas Xydas, David Tsi, Vladimir Gurevich, Mark Krichever, Imin Kao

CONCURRENT ENGINEERING: Research and Applications

Dynamic Taguchi Methods and Parameter Design as Applied in Barcode Scanning and Scanners

Nicholas Xydas,[1] David Tsi,[2] Vladimir Gurevich,[2] Mark Krichever[2] and Imin Kao[1,*]

[1]*Department of Mechanical Engineering, Stony Brook University*
[2]*Symbol Technologies, Inc., One Symbol Plaza, Holtsville, NY 11742-1300, USA*

Abstract: In this article, the dynamic Taguchi methodology is applied to the design of a barcode scanner. The concurrent engineering process involves a team of design and manufacturing engineers engaged in both hardware and software aspects of the product. The purpose of this experimental study is to determine the correlation between the outcomes of the conventional design and Taguchi optimization. The main contribution of this work in the design of scanners include: (a) application of the Taguchi methodology to yield an optimum design for scanning and comparing it to the analytical design, and (b) proving the existing opto-mechanical design to be optimum, within the signal processing capabilities. Experimental design using orthogonal arrays is established, and experiments of scanning on different barcode designs are conducted. The ideal function of the dynamic methodology is identified and the control and noise factors are chosen for the experimental design. The signal-to-noise (S/N) ratios and sensitivity are calculated using the equations of dynamic Taguchi methodology. Missing data in experiments, due to the combination of extreme ranges of design parameters, are treated by the sequential approximation method. A theoretical optimum unit is assembled and tested as confirmation of the experimental design, based on the response charts for both S/N ratio and sensitivity. The results of the confirmation experiment show that the performance of the scanner design, based on the criterion of the S/N ratios, has improved.

Key Words: Taguchi methods, dynamic S/N ratios, ideal function, barcode scanner, parameter design, sequential approximation.

1. Introduction

Taguchi methods have been successfully applied to various fields of product design and optimization. In [1], the methods were applied to optimize the numerical control (NC) machining process. The process developed reduced the standard deviation of machining to 1/10 of the original. In his paper, Wu [2] presented Taguchi methods in 'robust technology' research and development. Later in Ford body engineering department [3], Taguchi methods were applied to optimize the door sealing and minimize the closing effort of the automotive weatherstrip. Taguchi methods in the area of robotics were used by Gong and Kao [4] to improve the accuracy and repeatability of robot arms. The objective of this article is to introduce and apply quality engineering to the designing of scanner products. Quality engineering deals mostly with the method of how to measure the ability of a product or process performing its ideal function in a robust way. An ideal function is an ideally proportional relationship between the input signal and selected output. Among recent publications, the robust design technology based on Taguchi methodology was presented in [5]. The new 'Mahalanobis–Taguchi' system in applications of pattern recognition was introduced in [6,7] with case studies.

The concept of Taguchi methods is based on the parameter design and the application of the signal-to-noise (S/N) ratios [5–7]. The parameter design is a key to achieving low cost and high quality simultaneously. During the parameter design stage, the control and noise factors are identified. The control factors refer to the design parameters that we can control and will be assigned a two or three levels of design values during experimental design, while the noise factors refer to the factors that we cannot control or do not intend to control. These parameters are organized in a systematic way using the orthogonal array to conduct the experiment. The results of the experiments are calculated and compared via the S/N ratios. The S/N ratio is the measure of mean square deviation from the ideal function. Higher S/N ratios will promote the robustness of the design and should be used. The objective of the methodology that uses the dynamic S/N ratios is to achieve proportional input and output for appropriate

*Author to whom correspondence should be addressed.
E-mail: imin.kao@sunysb.edu

1063-293X/05/01 0069–12 $10.00/0 DOI: 10.1177/1063293X05050913

applications. In [8,9], Taguchi describes that the experimental design is used in three aspects of quality engineering: (1) to perform tuning to the target value, (2) to perform parameter design, and (3) to perform tolerance design.

In this article, we present the application of the Taguchi methods to a scanner product of Symbol Technology, Inc. A team of engineers and managers as well as researchers was assembled to work together for the concurrent engineering product analysis and development [10]. Four barcode symbols, used for the qualification tests of the barcode scanner, were chosen as targets. Code 1, 2, and 4 are binary codes, while code 3 is delta (see Table 4). The choice of the control and noise parameters was especially rigorous since it directly determines the outcome of the experiments. The ideal function for dynamic S/N ratio was chosen to be the linear relationship between the actual bar width versus the bar width measured by the scanner. Orthogonal arrays of L_{18} (inner array) and L_4 (outer array) types are used to conduct the experiments using quality engineering. Data processing and analysis was aided by the sequential approximation method to treat missing data in experiments, due to the combination of extreme ranges of control factors. The results show that the Taguchi methods can be applied to a complex system design such as the barcode scanner.

2. Methodology and Theoretical Background

A seven-step procedure has been summarized by Taguchi [9] to obtain dynamic S/N ratio as the most effective measure of robustness of the function. The seven steps are:

1. Identify the ideal function, specifying the input signal, output response, and their ranges.
2. If necessary, break down the system into several subsystems or modules, and specify the ideal function for each subsystem.
3. Predict critical noise factors that sway the actual function from the ideal, and specify the ranges of those noises.
4. Select several signal factor levels and a few noise levels. Usually it is preferable to choose only two points from the noise space by compounding all the selected noise factors into one compound noise factor with two extremes.
5. When the output of the function is not a continuous variable or it is not easy to measure, select some continuous design parameter to measure the magnitude of both signal and noises (operating window concept).
6. Conduct testing and obtain data on either the output or the selected parameter.
7. Calculate an appropriate S/N ratio considering possible tuning or calibration.

The equations for calculating the dynamic S/N ratios will be presented in more details in Section 4, when analyzing the data to obtain S/N ratios.

2.1 Orthogonal Arrays and Experimental Design

Typically for a system, there are many design parameters – some can be controlled by selecting design values within a certain range, while others cannot be controlled. If experiments are to be conducted according to the factorial design, the size of the experiment may be prohibitively high when the number of design variables exceeds five. In this regard, the orthogonal arrays are employed to conduct the minimum possible number of experiments [11,12]. In this case study, we choose the L_{18} array (see Table 10 in the Appendix), which has 18 experiments with eight control factors including, one two-level control factor, and seven three-level control factors. The overall orthogonal array (or the product array) consists of inner and outer arrays (see Table 10). The inner array includes all control factors; whereas, the outer array is composed of noise factors. In this article, a modified L_4 outer array (see Table 11) was chosen to include the compounded noise factors.

2.2 Control Factors and Noise Factors

The L_{18} inner array in Table 10 has eight control factors. The chosen control factors[1] are listed in Table 1. These control factors were carefully evaluated and chosen so as to ensure that we have considered all applicable and influential factors of this scanner design. The appropriate choice of performance-based parameters will shed physical insights of S/N ratio when data are analyzed.

Similarly, we identified the noise factors for the Taguchi experimental design, based on the design of the barcode scanner system. These noise factors are the ones that we either cannot control, or do not want to control. For example, the scanner is designed to be used in different parts of the world with conditions ranging from hot and humid to cold or frigid, and under different lighting situations. These are the expected noise

[1]The Taguchi methodology requires that the values of the levels of the chosen control factors be specified within the operating range of the system. Here, we use subscripts to denote the individual levels of the control parameters throughout this article to present a general methodology. In actual research and product development, the user will have to identify the actual control factors and establish their range of operation according to their specific application and engineering expertise. Once the ranges and levels of the control factors are established, as those in Table 1, experiments can be conducted to apply the Taguchi methods.

Table 1. List of the eight control factors employed in the design of the barcode scanner: factor A has two levels, while the remaining seven control factors have three levels.

Factor	Description	Levels		
A	The aperture edge geometry	A_1	A_2	N/A
B	Object distance (μ)	B_1	B_2	B_3
C	Cylindrical radius of mirror (mm)	C_1	C_2	C_3
D	Horizontal aperture size (in.)	D_1	D_2	D_3
E	Vertical aperture size (in.)	E_1	E_2	E_3
F	Scan amplitude (°)	F_1	F_2	F_3
G	Signal amplitude (V)	G_1	G_2	G_3
H	Bandwidth of filter (kHz)	H_1	H_2	H_3

Table 2. List of the compounded noise factors.

Factor	Description	Level 1	Level 2
X	Temperature/humidity	Low	High
Y	Ambient light and barcode quality	Room lighting/good	Sunlight/bad
Z	Barcode tilting	Tilting	No tilting

factors under which scanners need to perform successful scanning. In addition, these noise factors are combined for experimental convenience. With the objective of reducing the number of experiments, we adopted the compounding noise factors in an L_4 (see Table 11) outer array with the following three compound noise factors, as listed in Table 2.

2.3 Ideal Function and Measurements

In order to employ the dynamic Taguchi method [5], an ideal function needs to be identified, together with a reasonable measure that can be correlated to the quality of the system. The determination of an ideal function is based on the knowledge of the system and analysis. For the specific application presented in this article, we adopted the input as the widths of both the bars (black stripes of bars) and spaces (white space between bars) of the barcodes, and the output as the widths measured during successful scans. The ideal function, as defined by the Taguchi methods, is a proportional relationship between the input and the output. The dynamic ideal function

$$\mu = \beta M \tag{1}$$

is employed, where μ is the measured width (output), M is the widths of the bars and the stripes of the barcode (input), and β is the sensitivity. The goal is to promote the proportional relationship between the input and the output, so as to render the most robust scanning results using a set of control factors at chosen levels from the Taguchi experimental design.

The measurement of the output is expected to capture the significance of the S/N ratio, which represents the ratio between the useful signal to wasteful or unwanted signal. The signals $M_1, M_2, \ldots, M_n$ represent the input signal levels, which correspond to the widths of the measured bars and spaces of the barcodes. The value of n is determined by the total number of bars and spaces in the actual barcode used. Various symbologies of the standard barcodes are used. A software was developed to process the scanned data file and render the measurable widths for calculating S/N ratios.

3. Experimental Setup and Data Collection

In this section, we present the apparatus for the experiments and data collection.

3.1 Preparation of Experiments

For the L_{18} experiment, we need to assemble and test 18 scanners, based on the parameters established by the levels of control factors shown in Table 1. Each experiment represents one row in the L_{18} array and requires one scanner to be constructed according to the corresponding levels of parameters. The measurement in each row of the outer array is called a reading. The configuration of the 18 scanners assembled for the experiments is specified by the inner array in Table 10. Each scanner corresponds to the combination of control factor levels given in the matching line. For example, according to the L_{18} inner array, scanner #1 has the following configuration A_1, B_1, C_1, D_1, E_1, F_1, G_1, H_1. In order to reduce the time and the cost of the experiment, an L_4 outer array is used to combine the noise factors. A layout of the L_4 outer array for each experiment is shown in Tables 11 and 3. The four category columns in Table 3 ('Max Forward', 'Min Forward', 'Max Reverse', and 'Min Reverse') for each barcode represent the maximum and minimum values of barcode width readings in forward and reverse directions of scanning, respectively.

Four barcodes with different symbologies are used for conducting the experiments. The experimental setup is illustrated in Figure 1. A special fixture was designed and fabricated to simplify the testing routines and to make data collection consistent and efficient, as shown in the zoom-in window at the top of Figure 1. The sunlight simulator is used in experiments according to the L_4 array to control the intensity of sunlight in the testing environment. Four barcodes at different prescribed distances from the scanner are installed, together with an alignment target for calibration. The decoder

Table 3. Layout of the four L_4 outer arrays used for each of the four barcodes.

Noise Factors				**Max Forward**			**Min Forward**			**Max Reverse**			**Min Reverse**		
BARCODE #1 (99 bars and spaces)															
No.	X	Y	Z	M_1	···	M_{99}	M_{100}	···	M_{198}	M_{199}	···	M_{297}	M_{298}	···	M_{396}
N_1	1	1	1	$\mu_{1,1}$	···	$\mu_{1,99}$	$\mu_{1,100}$	···	$\mu_{1,198}$	$\mu_{1,199}$	···	$\mu_{1,297}$	$\mu_{1,298}$	···	$\mu_{1,396}$
N_2	1	2	2	$\mu_{2,1}$	···	···	···	···	···	···	···	···	···	···	$\mu_{2,396}$
N_3	2	1	2	$\mu_{3,1}$	···	···	···	···	···	···	···	···	···	···	$\mu_{3,396}$
N_4	2	2	1	$\mu_{4,1}$	···	···	···	···	···	···	···	···	···	···	$\mu_{4,396}$
BARCODE #2 (79 bars and spaces)															
No.	X	Y	Z	M_1	···	M_{79}	M_{80}	···	M_{158}	M_{159}	···	M_{237}	M_{238}	···	M_{316}
N_1	1	1	1	$\mu_{1,1}$	···	$\mu_{1,79}$	$\mu_{1,80}$	···	$\mu_{1,158}$	$\mu_{1,159}$	···	$\mu_{1,237}$	$\mu_{1,238}$	···	$\mu_{1,316}$
N_2	1	2	2	$\mu_{2,1}$	···	···	···	···	···	···	···	···	···	···	$\mu_{2,316}$
N_3	2	1	2	$\mu_{3,1}$	···	···	···	···	···	···	···	···	···	···	$\mu_{3,316}$
N_4	2	2	1	$\mu_{4,1}$	···	···	···	···	···	···	···	···	···	···	$\mu_{4,316}$
BARCODE #3 (115 bars and spaces)															
No.	X	Y	Z	M_1	···	M_{115}	M_{116}	···	M_{230}	M_{231}	···	M_{345}	M_{346}	···	M_{460}
N_1	1	1	1	$\mu_{1,1}$	···	$\mu_{1,115}$	$\mu_{1,116}$	···	$\mu_{1,230}$	$\mu_{1,231}$	···	$\mu_{1,345}$	$\mu_{1,346}$	···	$\mu_{1,460}$
N_2	1	2	2	$\mu_{2,1}$	···	···	···	···	···	···	···	···	···	···	$\mu_{2,460}$
N_3	2	1	2	$\mu_{3,1}$	···	···	···	···	···	···	···	···	···	···	$\mu_{3,460}$
N_4	2	2	1	$\mu_{4,1}$	···	···	···	···	···	···	···	···	···	···	$\mu_{4,460}$
BARCODE #4 (29 bars and spaces)															
No.	X	Y	Z	M_1	···	M_{29}	M_{30}	···	M_{58}	M_{59}	···	M_{87}	M_{88}	···	M_{116}
N_1	1	1	1	$\mu_{1,1}$	···	$\mu_{1,29}$	$\mu_{1,30}$	···	$\mu_{1,58}$	$\mu_{1,59}$	···	$\mu_{1,87}$	$\mu_{1,88}$	···	$\mu_{1,116}$
N_2	1	2	2	$\mu_{2,1}$	···	···	···	···	···	···	···	···	···	···	$\mu_{2,116}$
N_3	2	1	2	$\mu_{3,1}$	···	···	···	···	···	···	···	···	···	···	$\mu_{3,116}$
N_4	2	2	1	$\mu_{4,1}$	···	···	···	···	···	···	···	···	···	···	$\mu_{4,116}$

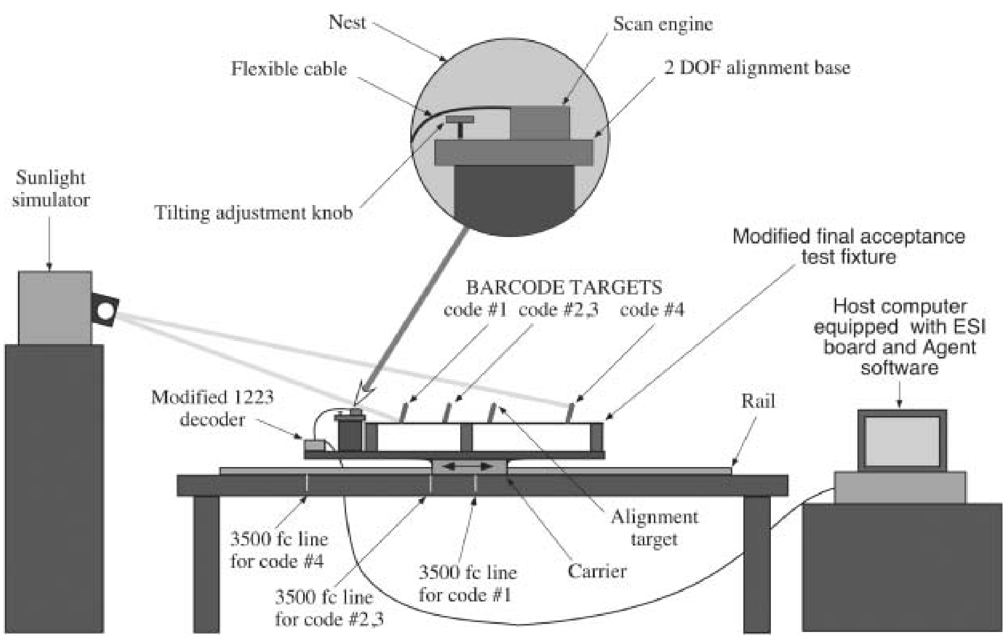

Figure 1. Experimental setup for measurement of scanning and data collection.

and the computer-based data acquisition system are used for data collection and subsequent analysis.

3.2 Experiments and Data Collection

The scanners were placed in an environmental chamber for 12 h at each environmental noise condition of temperature and humidity. Temperature and humidity stressing was executed for two extreme storage temperature and humidity levels, according to the L_4 design. After going through each environmental condition prescribed by the compound levels, the scanners were placed on the experimental fixture (Figure 1) to gather the scanning data immediately.

The measurements were taken at the ambient temperature, under both room lighting conditions and simulated sunlight conditions. Two qualities of barcodes were used, photographic and photocopied. For each of the four barcodes and each of the 18 experiments, measurements were taken, following the combination of the noise factors prescribed by the L_4 outer array. The entries of L_4 were used to assemble the four product arrays, like the one in Table 10. Because the dimension of the output arrays were huge, the entries are not listed individually in the tables. A computer program was written to handle the product arrays in analysis.

4. Data Processing and Analysis

The decoding of data files is done by using a custom-written software based on the decoding algorithm presented in [13]. The main features of the software include:

- Decoding of data files acquired during the experiments;
- Returning bar and space widths; and
- Printing maximum and minimum values of a successful scan.

The software is executed 288 times, corresponding to the equal number of data files generated by the data acquisition system. In order to capture the variation of the process, the minimum and maximum values of the readings for both directions are treated as distinct input data. These are denoted as the four category columns in Table 3. Therefore, the number of inputs for each barcode is equal to four times the number of bars and spaces i.e., Max Forward, Min Forward, Max Reverse, Min Reverse). Because of the large amount of data to be processed, the software has been developed to expedite the data processing as well as to minimize the possibility of processing errors. The decoding output is a matrix $4 \times N_b$, where N_b is the number of bars and spaces of the specific barcode. Table 4 lists the properties of the four barcodes used in the experiments.

Table 4. The four barcodes for measurement and analysis.

Barcode	Format	Number of Bars and Spaces
1	binary	99
2	binary	79
3	delta	115
4	binary	29

4.1 Equations for Analysis using the Dynamic Taguchi Method

In this article, the ideal function with proportion formulation between the input and the output, as that in Equation (1), is employed with the barcode widths as the input and the scanned widths as the output. In an ideal situation, the input and the output should be the same or be directly proportional to each other. The equations used to calculate the S/N ratios and sensitivity are presented in the following.

The sum of each input, Y_j, with j ranging from 1 to n, is

$$Y_j = \sum_{i=1}^{l} \mu_{i,j} \tag{2}$$

or in the expanded form

$$\begin{cases} Y_1 &= \mu_{1,1} + \mu_{2,1} + \mu_{3,1} + \cdots + \mu_{l,1} \\ Y_2 &= \mu_{1,2} + \mu_{2,2} + \mu_{3,2} + \cdots + \mu_{l,2} \\ \vdots & \\ Y_n &= \mu_{1,n} + \mu_{2,n} + \mu_{3,n} + \cdots + \mu_{l,n} \end{cases} \tag{3}$$

where $\mu_{i,j}$ is the measurement from experiments, as recorded in Table 3, l is the number of compound noises, and n is the number of inputs. Several 'S' values for various sums are obtained with

$$S_T = \mu_{1,1}^2 + \mu_{1,2}^2 + \cdots + \mu_{1,n-1}^2 + \mu_{1,n}^2 \tag{4}$$

$$S_\beta = \frac{1}{rr_0}(M_1 Y_1 + M_2 Y_2 + \cdots + M_n Y_n)^2 \tag{5}$$

$$S_L = \frac{1}{r}\left(L_1^2 + L_2^2 + \cdots + L_l^2\right) \tag{6}$$

where, $r = \sum_{j=1}^{n} M_j^2 = M_1^2 + M_2^2 + \cdots + M_n^2$, $r_0 = l$, Y_j is defined in Equation (2), and $L_i = \sum_{j=1}^{n} \mu_{i,j} M_j$. In addition, we define

$$S_{\beta\times N} = S_L - S_\beta \tag{7}$$

$$S_e = S_T - S_L = S_T - S_\beta - S_{\beta\times N} \tag{8}$$

$$S_N = S_T - S_\beta \tag{9}$$

The variability, which may be used as an indication of the quality of the product design, are defined as

$$V_e = \frac{S_e}{r_0(n-1)} \tag{10}$$

$$V_N = \frac{S_N}{r_0 n - 1} \tag{11}$$

Table 5. The S/N ratios and sensitivity, as calculated from the experimental data, for barcode #1 to #4.

	S/N Ratios				Sensitivity			
No.	**Code #1**	**Code #2**	**Code #3**	**Code #4**	**Code #1**	**Code #2**	**Code #3**	**Code #4**
1	60.1036	52.7546	55.8814	43.5728	−0.8832	−1.0859	0.0165	−0.0193
2	59.6634	54.0461	58.0768	47.6134	−0.8939	−0.9985	0.0712	−0.0145
3	63.8781	0	0	0	−0.7365	0	0	0
4	62.9955	54.8130	59.1846	0	−0.7954	−0.9698	0.0928	0
5	58.1536	0	0	40.5698	−0.9637	0	0	−0.1284
6	64.2086	57.2027	59.7733	0	−0.7557	−0.8509	0.1290	0
7	62.833	55.5908	58.7231	43.8158	−0.7928	−0.9159	0.0764	−0.1023
8	0	0	60.4925	46.5472	0	0	0.1207	−0.0522
9	61.026	53.7444	0	41.3056	−0.8459	−1.0004	0	−0.1306
10	61.5397	54.5482	57.5669	46.2400	−0.8292	−0.9648	0.0823	−0.0018
11	62.6732	55.0985	59.2219	52.1289	−0.7976	−0.9594	0.0722	−0.0003
12	60.1978	54.0865	0	43.7371	−0.8765	−0.9891	0	−0.0048
13	63.5798	55.4585	59.8541	50.4009	−0.7721	−0.9377	0.1018	−0.0007
14	59.8591	0	0	42.3823	−0.882	0	0	−0.0495
15	61.7817	54.8911	57.9232	47.6752	−0.8187	−0.9619	0.0660	−0.0158
16	62.0884	0	0	38.2143	−0.7972	0	0	−0.2608
17	61.2429	54.8938	57.8313	44.5048	−0.8515	−0.9560	0.0649	−0.0362
18	64.5725	0	60.8024	0	−0.7505	0	0.1126	0

Thus, the dynamic S/N ratio and sensitivity (the dynamic β) can be calculated, respectively, as follows

$$S/N = 10\log\left[\frac{(1/rr_0)(S_\beta - V_e)}{V_N}\right] \tag{12}$$

$$S = 10\log\left[\frac{1}{rr_0}(S_\beta - V_e)\right] \tag{13}$$

In this article, we use $l = 4$ and $n = 396$, 316, 460, and 116 for the four barcodes, respectively, based on the arrangement of the outer array. Equations (2)–(13) are applied to each barcode separately with different values of n. A numerical example for the calculation of S/N ratios and sensitivity is presented in Appendix B for the illustration of analysis. The results for each barcode are shown in Table 5.

4.2 Treatment of Missing Data in Experiments: Sequential Approximation

It is possible that some data in the designed experiments cannot be obtained because of the combination of the extreme range of control factors. Under such circumstances, we need to treat the missing data using the sequential approximation technique before the response table and charts for the S/N ratios and sensitivity can be obtained and plotted. The sequential approximation method employs successive iteration of S/N ratios (or sensitivity) with average values based on the S/N ratios associated with various levels of control factors. The iteration which updates the estimate of the S/N ratio or sensitivity continues until the value has converged. The convergence of such a method is generally very robust. The algorithm is best illustrated using an example with experimental data, as presented in Appendix C.

With the scanner design experiment at hand, we found that some of the scanners were unable to decode all or some of the symbols after environmental stressing. As a result, a total of 17 out of 72 S/N ratios and sensitivity values are missing. The missing data in Table 5 are indicated by zeros. Based on the data in Table 5, the algorithm of the sequential approximation is applied to the analysis of the data. An example of the application of the sequential approximation technique is illustrated in Appendix C, using the results of S/N ratios of barcode #1. After applying the sequential approximation, the missing data can be replaced by the new values. Table 6 lists the S/N ratios and sensitivity values of the individual barcodes, after applying the sequential approximation technique, as well as the overall values obtained by averaging the results of all four barcodes. The final response table of the Taguchi experimental design, based on the data in Table 6, can be obtained by employing the Taguchi methodology and averaging the data for each level of the control factors in Table 6. The response table of both the S/N ratios and sensitivity is in Table 7.

5. Results and Discussion

In this section, we analyze and discuss the results of the experimental design and confirmation run.

Table6. S/N ratios and sensitivity values for barcodes (Code #1 to #4), after applying the sequential approximation technique to replace the missing experimental data.

	S/N Ratios					Sensitivity				
No	**Code #1**	**Code #2**	**Code #3**	**Code #4**	**Avg.**	**Code #1**	**Code #2**	**Code #3**	**Code #4**	**Avg.**
1	60.10	52.75	55.88	43.57	53.08	−0.8832	−1.0859	0.01659	−0.01933	−0.4930
2	59.66	54.05	58.08	47.61	54.85	−0.8939	−0.9985	0.07127	−0.01455	−0.4589
3	63.88	55.72	60.24	51.17	57.75	−0.7365	−0.9218	0.11810	−0.02942	−0.3924
4	62.99	54.81	59.18	52.06	57.26	−0.7955	−0.9698	0.09285	−0.00184	−0.4186
5	58.15	53.82	58.14	40.57	52.67	−0.9638	0.9730	0.06687	−0.12850	−0.4997
6	64.21	57.20	59.77	46.27	56.86	−0.7558	−0.8510	0.12906	0.04260	−0.3588
7	62.83	55.59	58.72	43.82	55.24	−0.7928	−0.9159	0.07640	−0.10230	−0.4337
8	62.46	55.17	60.49	46.55	56.17	−0.7932	−0.8552	0.12071	−0.05230	−0.3950
9	61.03	53.74	57.49	41.31	53.39	−0.8460	−1.0005	0.04239	−0.13060	−0.4837
10	61.54	54.55	57.57	46.24	54.97	−0.8293	−0.9648	0.08240	−0.00188	−0.4284
11	62.67	55.10	59.22	52.13	57.28	−0.7976	−0.9594	0.07221	−0.00034	−0.4213
12	60.20	54.09	57.73	43.74	53.94	−0.8766	−0.9891	0.04980	−0.00488	−0.4552
13	63.58	55.46	59.85	50.40	57.32	−0.7721	−0.9377	0.10186	0.00079	−0.4018
14	59.86	55.94	58.26	42.38	54.11	−0.8821	−0.9116	0.08909	−0.04950	−0.4385
15	61.78	54.89	57.92	47.67	55.57	−0.8187	−0.9620	0.06606	−0.01590	−0.4326
16	62.09	55.36	57.75	38.21	53.35	−0.7973	−0.8973	0.07270	−0.26080	−0.4707
17	61.24	54.89	57.83	44.50	54.62	−0.8516	−0.9560	0.06491	−0.03620	−0.4447
18	64.57	54.04	60.80	46.41	56.46	−0.7505	−0.8959	0.11261	−0.09140	−0.4063

Table 7. Response table for the S/N ratios and sensitivity.

	S/N Ratios			Sensitivity		
No.	**Level 1**	**Level 2**	**Level 3**	**Level 1**	**Level 2**	**Level 3**
A	55.25	55.29	n/a	−0.4371	−0.4333	n/a
B	55.31	55.63	54.87	−0.4415	−0.4250	−0.4390
C	55.21	54.95	55.66	−0.4410	−0.4430	−0.4215
D	55.20	55.08	55.54	−0.4490	−0.4426	−0.4140
E	55.50	55.19	55.12	−0.4253	−0.4385	−0.4418
F	55.33	55.17	55.31	−0.4247	−0.4391	−0.4417
G	53.42	55.35	57.04	−0.4735	−0.4262	−0.4059
H	54.82	55.51	55.49	−0.4425	−0.4325	−0.4305

5.1 Results and Confirmation Run

The response charts can be plotted, based on the results of the S/N ratios and sensitivity in Table 7. Figure 2 plots the S/N ratios of the levels of the eight control factors, while Figure 3 illustrates the sensitivity.

From the response tables and charts, we find that the most influential control factor is the signal amplitude (factor G), while the least influential is the aperture shape (factor A). The shapes of the response chart reveal that there are interactions among the control factors. From the charts, the optimum design configuration is determined by the levels of the factors with the highest S/N ratios. Thus, the optimal configuration is found to be $A_2B_2C_3D_3E_1F_1G_3H_2$. Note that the signal amplitude also has the largest influence on the sensitivity.

Based on this configuration, the optimal unit was assembled and tested. During the testing of the optimal unit, the limitation on the performance of the scanner was observed when using signal amplitude level three (G_3). Therefore, the intermediate signal amplitude level value was selected as the nominal (which is at G_2 level), and the optimal configuration was revised to $A_2B_2C_3D_3E_1F_1G_2H_2$. This optimum unit was chosen and assembled to perform the confirmation run. In addition, one nominal unit based on the current barcode scanner design was also assembled for comparison. Following the same procedure for experiments, the confirmation run was conducted, with results summarized in Tables 8 and 9.

5.2 Discussion

The experimental results of the confirmation run of the optimum design agree with the estimated S/N ratios in general. As shown by the S/N ratios in Tables 8 and 9 of the confirmation run, the predicted and the confirmed values for both optimal and nominal designs are very much in agreement. The absolute difference between the predicted and confirmed values for the optimal configuration is 0.0789 dB (see Table 9). The accuracy of prediction is 99.86%. Similarly, the difference for the nominal case is 1.631 dB and the accuracy of prediction 97.04%. The accuracy of the results is an indication of the experimental consistency.

Because each of the four barcodes has different optimal conditions, the optimal unit is a trade-off among all four optimal designs. The experimental results of S/N ratios in Table 8 indicate that the optimal scanner unit performs better for scanning the barcodes #1 and #2,

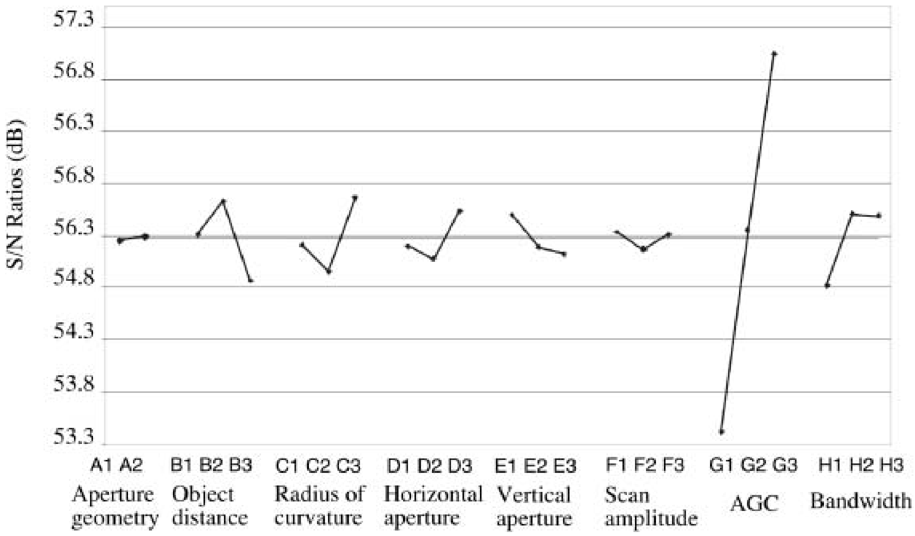

Figure 2. Response chart for the S/N ratios.

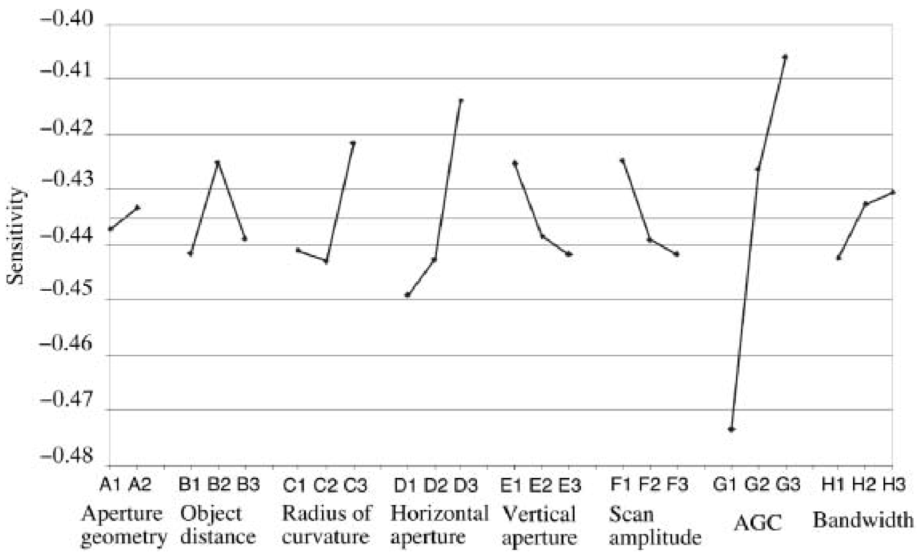

Figure 3. Response chart for the sensitivity.

Table 8. Confirmation run: the S/N ratios for the nominal and optimal designs.

Code #1		Code #2		Code #3		Code #4		Average		Predicted	
Nom.	**Opt.**	**Nom.**	**Opt.**	**Nom.**	**Opt.**	**Nom.**	**Opt.**	**Nom.**	**Opt.**	**Nom.**	**Opt.**
63.44	64.54	55.95	57.51	59.59	59.41	48.37	45.89	56.84	56.84	55.21	56.92

Table 9. Comparison between the optimal and nominal units.

	Optimal					Nominal		
	$A_2B_2C_3D_3E_1F_1G_2H_2$					$A_2B_2C_2D_2E_3F_2G_2H_2$		
	Predicted	**Confirmed**	**Δ**	**Avg. Design**	**Improvement**	**Predicted**	**Confirmed**	**Δ**
S/N	56.92	56.84	−0.0789	55.27	1.566	55.21	56.84	1.631

poorer for barcode #4, and nearly the same for barcode #3. The results are obtained by conducting range test on both the optimal and nominal scanner units. The experimental results, as shown in Table 9, give an overall S/N ratio of 56.84 – a good agreement with the predicted value of 56.92. This suggests that the confirmation experiment, under the designated levels, is consistent with the prediction of the L_{18} experiments. Furthermore, the results of the confirmation run show that the performance, based on the S/N ratios, is improved for barcodes #1 and #2, but deteriorated for barcode #4. The results also suggest that barcodes of different optimal conditions may favor one type of scanner instead of the other.

In addition, we discovered that signal amplitude level three (G_3) did not result in successful scans on barcode #4, although it worked for the other three barcodes. Subsequent analysis shows that the threshold value employed in the software decoding, which was not included as a control parameter in the L_{18} experiments, was probably too low to decode the signal under magnified signal amplitude level three during the experiments. At the time of the experimental design, the software parameter of the threshold of signal processing for decoding was not an option for control factor. It is concluded from this research study that such a parameter has to be included in future designs of experiments, in addition to the chosen parameters of hardware design. Furthermore, one other reason why the optimal unit makes only incremental improvements to the barcode scanner design is because the existing scanner design has already been optimized opto-mechanically and performs very well. This observation was validated by the small variability values in V_e, obtained in the data analysis. Hence, improvement can only be made incrementally on this barcode scanner design, and sometimes a trade-off of performance on different barcode designs may be required, as presented in the preceding analysis.

6. Conclusions

In this article, we apply the dynamic Taguchi methodology to the design of the barcode scanner, and conduct the experimental design using the L_{18} orthogonal array. The S/N ratios are calculated using the equations of the dynamic S/N ratios. Missing data, due to the combination of extreme ranges of control factors, are treated by the sequential approximation method. A theoretical optimum unit was assembled, and the confirmation run conducted. The results show very good agreement between the theoretical and experimental results.

Based upon the results of the experiments, we show that the Taguchi methodology yields a similar optimum design as the analytical one, and prove that the existing opto-mechanical design is optimum, within the signal processing capabilities. However, limitation of the methodology as applied to the design of the barcode scanner is found in one standard barcode, though two other barcodes show improved scanning performance as predicted by the S/N ratios. All control factors considered are parameters related to hardware, while the scanning data processing is done in software. In the future application of Taguchi methods to this type of application, the critical software parameters pertaining to signal processing may need to be included. Nevertheless, the analysis of Taguchi Methods on this barcode scanner design reveals that the existing design has very good quality, as evident by the small variability values obtained.

This collaborative project also enjoys a team of concurrent engineering from design to manufacturing, as well as hardware and software engineers, who worked on the application of the Taguchi methods to the design of scanners.

Acknowledgments

The authors would like to thank Professor Yuin Wu for his valuable advice and suggestions throughout this work. Mr. Irwin Cohen of the division of analog electronics and Mr. Joe Cai of the software division have contributed during the design stage. They would also like to thank Ms. Linda True and Mr. Erick Arango from manufacturing and quality engineering who participated in the early stage of the design work. The project has received enthusiastic support since its beginning from Dr. Satya Sharma, as well as Mr. Boris Metlisky. Without their support, this work would not have been realized. The research project was sponsored by Symbol Technologies, Inc.

Appendices

A. The L_{18} ($2^1 3^7$) and L_4 (2^3) Orthogonal Arrays

The inner array L_{18} and the outer array L_4 employed in this paper are tabulated in Tables 10 and 11. The choice and arrangement of the control factors and noise factors are presented in Section 2.2.

B. Example for the Calculation of S/N Ratios and Sensitivity

Using the experimental data in Table 12, we illustrate with a numerical example, the calculation of the S/N ratios and sensitivity. First of all, we have $r_0 = l = 4$ and $n = 396$ for barcode #1. The calculation

***Table 10.** Product array having the L_{18} inner orthogonal array with eight control factors attached to the left side. The first factor, A , is two-level and the remaining seven control factors, B to H, three-level. M is the input, N is the compounded noise, μ is the measured output and n is the number of inputs.*

Inner Array									M_1				…	M_n			
No.	A	B	C	D	E	F	G	H	N_1	N_2	N_3	N_4	…	N_1	N_2	N_3	N_4
1	1	1	1	1	1	1	1	1	$\mu_{1,1}$	$\mu_{2,1}$	$\mu_{3,1}$	$\mu_{4,1}$	…	$\mu_{1,n}$	$\mu_{2,n}$	$\mu_{3,n}$	$\mu_{4,n}$
2	1	1	2	2	2	2	2	2	…	…	…	…	…	…	…	…	…
3	1	1	3	3	3	3	3	3									
4	1	2	1	1	2	2	3	3									
5	1	2	2	2	3	3	1	1									
6	1	2	3	3	1	1	2	2									
7	1	3	1	2	1	3	2	3									
8	1	3	2	3	2	1	3	1									
9	1	3	3	1	3	2	1	2									
10	2	1	1	3	3	2	2	1									
11	2	1	2	1	1	3	3	2									
12	2	1	3	2	2	1	1	3									
13	2	2	1	2	3	1	3	2									
14	2	2	2	3	1	2	1	3									
15	2	2	3	1	2	3	2	1									
16	2	3	1	3	2	3	1	2									
17	2	3	2	1	3	1	2	3									
18	2	3	3	2	1	2	3	1	…	…	…	…	…	…	…	…	…

***Table 11.** L_4 outer orthogonal array with three compound noise factors, each having two levels. This L_4 array is used to render compound noise factors in experiments.*

No.	X	Y	Z
1	1	1	1
2	1	2	2
3	2	1	2
4	2	2	1

in this appendix follows Equations (2)–(13). We first obtain

$$r = 0.0049^2 + 0.0126^2 + \cdots + 0.0049^2 = 0.02562$$

$$\begin{cases} Y_1 = 0.0064 + 0.0064 + 0.0068 + 0.0061 = 0.0256 \\ \vdots \\ Y_{396} = 0.0057 + 0.0066 + 0.0064 + 0.0061 = 0.0249 \end{cases}$$

The terms of the linear equations are calculated

$$\begin{cases} L_1 = 0.0064 \times 0.0049 + \cdots + 0.0057 \times 0.0049 = 0.023336 \\ \vdots \\ L_4 = 0.0061 \times 0.0049 + \cdots + 0.0061 \times 0.0049 = 0.023100 \end{cases}$$

The various S values and variability are

$$S_T = 0.0049^2 + 0.0126^2 + \cdots + 0.0049^2 = 0.08489 \quad (f = 1584)$$

$$S_\beta = \frac{1}{0.256 \times 4}(0.0049 \times 0.0256 + \cdots + 0.0049 \times 0.0249)^2 = 0.083626 \quad (f = 1)$$

$$S_L = \frac{0.0233^2 + 0.0229^2 + 0.0232^2 + 0.231^2}{0.0256} = 0.083626 \quad (f = 4)$$

$$S_{\beta \times N} = 0.0836260314 - 0.0836260000 = 3.141 \times 10^{-6} \quad (f = 3)$$

$$S_e = 0.08489 - 0.08363 - 3.140883 \times 10^{-6} = 0.001257 \quad (f = 1580)$$

$$S_N = 0.08489 - 0.08363 = 0.00126 \quad (f = 1583)$$

$$V_e = \frac{0.001257}{4(396 - 1)} = 7.96 \times 10^{-7}$$

$$V_N = \frac{0.00126}{4 \times 396 - 1} = 7.96 \times 10^{-7}$$

The parameter 'f' in the above equations denotes the degree of freedom of the data in each applicable

Table 12. L_4 outer arrays with data from the first experiment (the first row of the L_{18} array) of the barcode #1.

	Barcode #1 (99 bars and spaces)											
	Max Forward			**Min Forward**			**Max Reverse**			**Min Reverse**		
No.	M_{11}	···	M_{99}	M_{100}	···	M_{198}	M_{199}	···	M_{297}	M_{298}	···	M_{396}
N_1	0.0064	···	0.0062	0.0060	···	0.0059	0.0049	···	0.0060	0.0047	···	0.0057
N_2	0.0064	···	0.0067	0.0059	···	0.0058	0.0049	···	0.0085	0.0046	···	0.0066
N_3	0.0068	···	0.0063	0.0063	···	0.0057	0.0049	···	0.0070	0.0047	···	0.0064
N_4	0.0061	···	0.0063	0.0056	···	0.0057	0.0047	···	0.0067	0.0046	···	0.0061

Table 13. The list of the 18 S/N ratios of barcode #1 from experiments (see the first data column of Table 5). The entry of '0' S/N ratio in the eighth experiment indicates a missing S/N value corresponding to the missing experimental data.

No.	**1**	**2**	**3**	**4**	**5**	**6**	**7**	**8**	**9**
S/N	60.10	59.66	63.88	63.00	58.15	64.21	62.83	0	61.03
No.	**10**	**11**	**12**	**13**	**14**	**15**	**16**	**17**	**18**
S/N	61.54	62.67	60.20	63.58	59.86	61.78	62.09	61.24	64.57

calculation. Therefore, the dynamic S/N ratio and the sensitivity (dynamic β) are

$$\eta = 10\log\left[\frac{(1/0.02562 \times 4)(0.083626 - 7.96 \times 10^{-7})}{7.96 \times 10^{-7}}\right]$$
$$= 60.10$$
$$S = 10\log\left[\frac{1}{0.02562 \times 4}(0.083626 - 7.96 \times 10^{-7})\right]$$
$$= -0.8832$$

C. Example of Treating Missing Data: *Sequential Approximation*

In this section, the sequential approximation method will be illustrated using the example of the results of experiments on the barcode #1.

The missing data is at experiment eight, where the S/N ratio is recorded as '0' in Table 13. The average of the remaining 17 nonzero S/N ratios, $\bar{\eta}$, is calculated as follows:

$$\bar{\eta} = \frac{1}{17}(60.10 + 59.66 + \cdots + 61.24 + 64.57)$$
$$= 61.79\,\text{dB} \tag{14}$$

As the initial value for the first iteration in applying the sequential approximation method, the value of $\bar{\eta}$ obtained in Equation (14) will be applied to replace the missing data. Using the new value, $\bar{\eta} = 61.79$ for the eighth data, the S/N ratios for each level of the control factors are calculated and tabulated in the response table, as shown in Table 14.

Table 14. Response table obtained after the first iteration.

Factor	Level 1	Level 2	Level 3
A	61.63	61.95	n/a
B	62.19	61.76	62.26
C	61.64	60.56	62.61
D	61.64	61.50	62.23
E	62.38	61.42	61.57
F	61.85	61.61	61.90
G	60.24	61.88	63.25
H	61.32	62.21	61.83

In order to continue the iteration to the next estimate of the S/N ratio for the missing data, we find the difference between the high and low S/N ratios associated with the eight factors, A–H, and order them based on the magnitude of the difference/gap. This is listed in Table 15. Next, we pick half of the factors with the largest gap or difference (G, C, E, B, in this case). These four factors have a larger influence on the outcome of the sequential approximation. The estimate of the missing data for the next iteration will be adopted as the difference between the sum of the four control factors[2] corresponding to the specific levels of the control factors of eighth data entry,[3] and three times the grand average, $\overline{T}$. That is, the estimate of the S/N ratio for the next iteration is

$$\eta_8 = \overline{G}_3 + \overline{C}_2 + \overline{E}_2 + \overline{B}_3 - 3\overline{T}$$

[2]The four control factors G, C, E, and B have the largest effect (gap) listed in Table 15.
[3]According to the L_{18} array in Table 10, the eighth data entry has the following arrangement of levels of control factors: $A_1B_3C_2D_3E_2F_1G_3H_1$.

Table 15. High–low S/N ratios for the eight control factors.

	High		Low		
Factor	**Level**	**S/N ratio**	**Level**	**S/N ratio**	**Gap**
G	3	63.25	1	60.24	3.01
C	3	62.61	2	60.56	2.05
E	1	62.38	2	61.42	0.96
B	3	62.26	1	61.34	0.92
H	2	62.21	1	61.32	0.89
D	3	62.23	2	61.50	0.73
A	2	61.95	1	61.63	0.32
F	3	61.90	2	61.61	0.29

Table 16. Results after seven iterations. The S/N ratio for the missing experiment converges to the final value of 62.46.

Iteration	S/N ratio	Convergence (%)
1	62.12	0.5448
2	62.29	0.2709
3	62.38	0.1350
4	62.42	0.0674
5	62.44	0.0337
6	62.45	0.0168
7	62.46	0.0084

where the grand average of the 18 S/N ratios from Table 13, with the eighth S/N values replaced by the new value $\bar{\eta}$=61.79, is

$$\overline{T} = \frac{1}{N}\sum_{i=1}^{N} \eta_i$$

with $N = 18$ for L_{18} orthogonal array employed in this experimental design.

Substituting numerical values into Equations (15) and (16), we obtain

$$\overline{T} = \frac{1}{18}(60.10 + 59.66 + \cdots + 61.79 + \cdots + 61.24 + 64.57)$$
$$= 61.79\,\mathrm{dB}$$
$$\eta_8 = 63.25 + 60.56 + 61.42 + 62.26 - 3 \times 61.79$$
$$= 62.12$$

The new value of $\eta_8 = 62.12$ will be adopted for the next iteration. The same iteration procedure will be repeated until convergence is reached; that is, when the S/N ratio do not change much with further iteration. Repeating this iterative process until convergence is reached, the S/N ratio, η_8 , can be obtained to replace the missing data entry, as listed in Table 16.

If more than one experimental data are missing (for example, the S/N ratios of barcode #2 in Table 5), the same procedure that was illustrated in the example above can be employed on all missing data entries. Once a data entry has converged, the iteration for that particular data can be stopped, while proceeding with the remaining data entries until they all converge.

References

1. Miura, Y. and Ueno, K. (1992). NC Machining Technology Development—NC Machining for High Frequency Heat Treatment, In: *Tenth Annual Taguchi Symposium*, ASI, Oct. 12–14, pp. 345–352.
2. Wu, Y. (1993). Robust Technology Development: Can We Reduce R&D Cycle Time to One-third?, American Supplier Institute, Technical Report.
3. Pack, J., Kovch, I., Machin, R., Zhou, J.H. and Riley, S. (1993). Systematic Design of Automotive Weatherstrips using Taguchi Robust Design Methods, In: *Eleventh Annual Taguchi Symposium*, ASI, November 1993, pp. 103–123.
4. Gong, C. and Kao, I. (1997). Design for Accuracy and Repeatability for Robots using Taguchi Methods, *The Journal of Concurrent Engineering Research and Applications*, **5**: 263–278.
5. Wu, Y. and Wu, A. (2000). *Taguchi Methods for Robust Design*, ASME Press.
6. Taguchi, G., Chowdhury, S. and Wu, Y. (2001). *The Mahalanobis-Taguchi System*, McGraw Hill.
7. Taguchi, G. and Jugulum, R. (2002). *The Mahalanobis-Taguchi Strategy: A Pattern Technology System*, Wiley.
8. Taguchi, G. (1993). *Taguchi on Robust Engineering*, ASME Press.
9. Taguchi, G. (1995). Difference between Science and Engineering, Signal-to-noise Ratio, ASI, Tech. Report.
10. Prasad, B. (1996). *Concurrent Engineering Fundamentals*, *Integrated Product and Process Organization*, Vol. 1, Upper Saddle River, New Jersey: Prentice Hall.
11. Taguchi, G. (1991). *System of Experimental Design*, Vols. 1 and 2, Dearborn, Michigan: Quality Resources.
12. Taguchi, G. and Konishi, S. (1992). *Taguchi Methods Research and Development, Quality Engineering Series*, Vol. 1, ASI Press.
13. Cai, Z. (1994). A New Decode Algorithm for Binary Bar Codes, *Pattern Recognition Letters*, **15**: 1191–1199.